Last Glacial Maximum CO2 and δ13C successfully reconciled

Article

Published Version

Last Glacial Maximum CO_2 and $\delta^{13}C$ successfully reconciled

N. Bouttes,[1] D. Paillard,[1] D. M. Roche,[1,2] V. Brovkin,[3] and L. Bopp[1]

Received 29 June 2010; revised 30 November 2010; accepted 14 December 2010; published 25 January 2011.

[1] During the Last Glacial Maximum (LGM, ~21,000 years ago) the cold climate was strongly tied to low atmospheric CO_2 concentration (~190 ppm). Although it is generally assumed that this low CO_2 was due to an expansion of the oceanic carbon reservoir, simulating the glacial level has remained a challenge especially with the additional $\delta^{13}C$ constraint. Indeed the LGM carbon cycle was also characterized by a modern-like $\delta^{13}C$ in the atmosphere and a higher surface to deep Atlantic $\delta^{13}C$ gradient indicating probable changes in the thermohaline circulation. Here we show with a model of intermediate complexity, that adding three oceanic mechanisms: brine induced stratification, stratification-dependant diffusion and iron fertilization to the standard glacial simulation (which includes sea level drop, temperature change, carbonate compensation and terrestrial carbon release) decreases CO_2 down to the glacial value of ~190 ppm and simultaneously matches glacial atmospheric and oceanic $\delta^{13}C$ inferred from proxy data. LGM CO_2 and $\delta^{13}C$ can at last be successfully reconciled. **Citation:** Bouttes, N., D. Paillard, D. M. Roche, V. Brovkin, and L. Bopp (2011), Last Glacial Maximum CO_2 and $\delta^{13}C$ successfully reconciled, *Geophys. Res. Lett.*, *38*, L02705, doi:10.1029/2010GL044499.

1. Introduction

[2] The Last Glacial Maximum (LGM, ~21,000 years ago) was characterized by a cold climate (−2 to −6°C in the surface Southern Ocean [*MARGO Project Members*, 2009]) associated with major northern hemisphere ice sheets covering large parts of Europe and North America [*Peltier*, 2004]. As it constitutes a different climate from the pre-industrial (PI) and is fairly well documented, it has been explored in many modeling studies and is now considered as a case study for coupled climate models used for anthropogenic climate change projections. These studies show that the low glacial atmospheric CO_2 (~190 ppm compared to 280 ppm during the pre-industrial) inferred from ice core data [*Monnin et al.*, 2001] plays a crucial role in explaining the cold climate [*Jahn et al.*, 2005]. Yet, although the Southern Ocean appears to be key in such changes [*Fischer et al.*, 2010; *Sigman et al.*, 2010], no complete explanation has been put forward that could both account for this low glacial CO_2 [*Archer et al.*, 2000; *Sigman and Boyle*, 2000] and the $\delta^{13}C$ values in the ocean and atmosphere [*Brovkin et al.*, 2007; *Tagliabue et al.*, 2009; *Bouttes et al.*, 2010]. Indeed the glacial oceanic $\delta^{13}C$ distribution was also changed [*Duplessy et al.*, 1988; *Curry and Oppo*, 2005], particularly with a higher surface (−2000 m to 0 m) to deep (−5000 m to −3000 m) gradient ($\Delta\delta^{13}C_{ocean}$ of ~1.4‰ in the Atlantic compared to ~0.6‰ in the modern ocean), while the $\delta^{13}C_{atm}$ level is close to the preindustrial one (~ −6.45‰) [*Lourantou et al.*, 2010]. Only box models could account for such changes [*Köhler et al.*, 2005, 2010; *Lourantou et al.*, 2010]. Yet, because of their simplicity, some mechanisms like oceanic circulation changes were imposed and their dynamics could not be tested.

[3] Out of the three global carbon reservoirs (atmosphere, terrestrial biosphere and ocean), proxy data indicate that two were smaller during the LGM. Atmospheric CO_2 was lower [*Monnin et al.*, 2001] and the terrestrial vegetation was reduced by at least several hundred GtC [*Bird et al.*, 1994; *Crowley*, 1995]. Consequently, the ocean should contain the glacial excess of carbon. Modeling studies have shown that a greatly stratified glacial ocean with lower SSTs could get towards the glacial values for the carbon cycle [*Toggweiler*, 1999; *Paillard and Parrenin*, 2004; *Brovkin et al.*, 2007; *Bouttes et al.*, 2009; *Tagliabue et al.*, 2009; *Bouttes et al.*, 2010]. In particular, when deep oceanic stratification is reached through enhanced brine formation (saline water released by sea ice formation that can rapidly sink towards the deep ocean), simulations can simultaneously reduce atmospheric CO_2 and increase $\Delta\delta^{13}C_{ocean}$ in the Atlantic [*Bouttes et al.*, 2010].

[4] Other mechanisms have been studied such as carbonate compensation [*Broecker and Peng*, 1987; *Brovkin et al.*, 2007] or iron fertilization [*Martin*, 1990; *Bopp et al.*, 2003; *Brovkin et al.*, 2007; *Tagliabue et al.*, 2009]. The carbonate compensation mechanism acts as an amplifier of the ocean carbon uptake or loss. It tends to restore the initial oceanic $[CO_3^{2-}]$ through changes in the sediment dissolution. Iron fertilization can take place in regions of High Nutrients Low Chlorophyll (HNLC) where the biological production is limited by iron (such as in the Southern Ocean). The supply of iron through dust transport and deposition during the LGM stimulates marine biology whose uptake of carbon increases. However, these mechanisms that alone can not account for the entire glacial carbon cycle values were not tested yet in conjunction with the brine mechanism.

[5] Here we show that we can finally reach simultaneously the glacial atmospheric CO_2 level, $\delta^{13}C_{atm}$ and $\Delta\delta^{13}C_{ocean}$ values with a combination of three main mechanisms when carbonate compensation is considered: brine induced stratification, stratification-dependant diffusion and iron fertilization.

2. Methods

[6] We use the CLIMBER-2 coupled intermediate complexity model [*Petoukhov et al.*, 2000] which is well suited to

[1]Laboratoire des Sciences du Climat et de l'Environnement, IPSL/CEA-CNRS-UVSQ, Gif-sur-Yvette, France.
[2]Section Climate Change and Landscape Dynamics, Faculty of Earth and Life Sciences, Vrije Universiteit Amsterdam, Amsterdam, Netherlands.
[3]The Land in the Earth System, Max-Planck-Institute for Meteorology, Hamburg, Germany.

0094-8276/11/2010GL044499

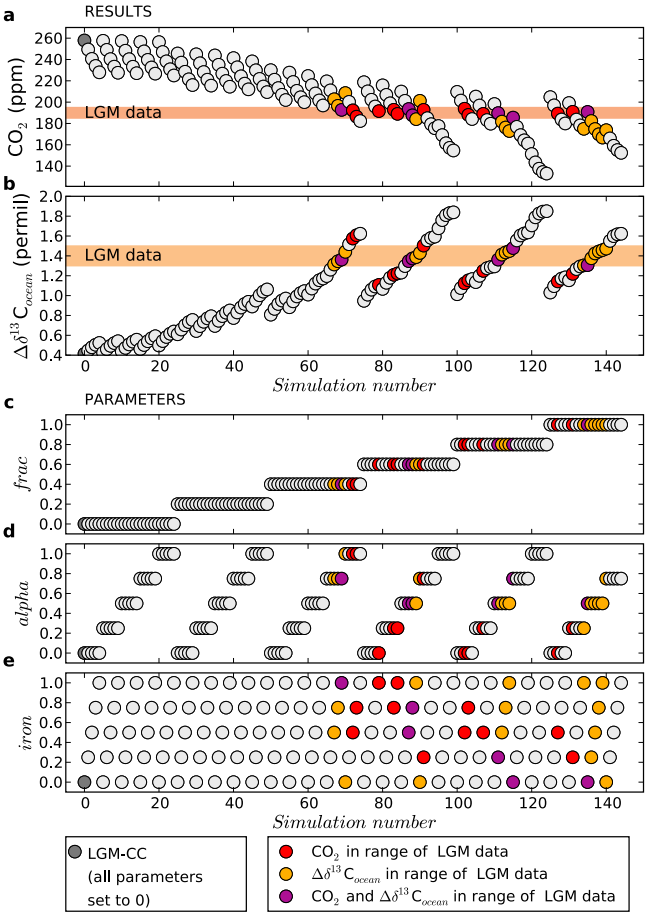

Figure 1. (a) Atmospheric CO_2 (ppm) and (b) $\Delta\delta^{13}C_{ocean}$ (‰) ($\delta^{13}C$ gradient in the Atlantic between the surface (0 to −2000 m) and the bottom (−3000 m to −5000 m)) for glacial simulations with brines, stratification-dependant diffusion and iron fertilization (carbonate compensation is included). The three varying parameters are: (c) *frac* (brine mechanism), (d) *alpha* (stratification-dependant diffusion) and (e) *iron* (iron fertilization). *LGM-CC* is the simulation with *frac* = *iron* = *alpha* = 0. Simulations that match the LGM data are highlighted with colors.

realize a large number of runs that are long enough to reach an equilibrium for the carbon cycle. Simulations were run for 50,000 years, but most of the CO_2 changes are reached by 10,000 years (less than 7 ppm change after 10,000 years). CLIMBER-2 includes a model of deep ocean carbonate sediments necessary to estimate the effect of carbonate compensation [*Archer*, 1991; *Brovkin et al.*, 2007]. The LGM conditions imposed are the glacial solar insolation [*Berger*, 1978], ice sheets [*Peltier*, 2004], and atmospheric CO_2 [*Monnin et al.*, 2001] for the radiative code (190 ppm, not used in the carbon cycle part of the model). To account for the ~120 m sea level fall, salinity and nutrient mean concentrations are increased by 3.3%. With these glacial conditions, despite the colder temperature and less intense thermohaline circulation, atmospheric CO_2 increases to 298 ppm (*LGM* simulation) mainly because of the reduced terrestrial biosphere (loss of 640 GtC compared to the pre-industrial). When carbonate compensation is included (*LGM-CC*) CO_2 decreases to 257 ppm as the carbonate compensation mechanism amplifies the oceanic uptake of carbon, which was previously analyzed in more detail [*Brovkin et al.*, 2007]. Further to carbonate compensation, three mechanisms are tested: the brine mechanism, iron fertilization and stratification-dependant diffusivity.

[7] The brine mechanism is a simple parameterization of the deep sink linked to the release of very salty water (brines) during the formation of sea ice [*Bouttes et al.*, 2010]. In the standard version of CLIMBER-2, the flux of salt released into the ocean is diluted in the first oceanic cell which is quite big due to the coarse resolution. Yet, as brines are very dense because of the high salinity, they should rapidly sink to the deep ocean favored by the glacial conditions in the Southern Ocean. This brine sink has been parameterized in CLIMBER-2 [*Bouttes et al.*, 2010]. The relative importance of the brine mechanism is set by the parameter *frac*, which is the fraction of salt released by sea ice formation that sinks to the bottom of the ocean. The rest of the salt (1 − *frac*) is diluted in the corresponding surface oceanic cell. When *frac* = 0 no salt sinks to the abyss (standard simulation), whereas *frac* = 1 is the maximum effect when all the rejected salt sinks to the bottom of the ocean. This mechanism was shown to result in a net glacial CO_2 decrease with a maximum drop of 52 ppm and increased Atlantic $\Delta\delta^{13}C_{ocean}$ (1.2‰) (*LGM-brines*).

[8] Iron fertilization is taken into account in the model by forcing biology to use a fraction (parameter *iron*) of the nutrients that would otherwise be left in the Atlantic and Indian sectors of the Sub-Antarctic surface ocean (30°S to 50°S) [*Brovkin et al.*, 2007]. The *iron* parameter represents the importance of iron fertilization. It can vary between 0 (no iron fertilization) and 1 (maximum iron fertilization, all nutrients in the area are consumed).

[9] Finally the stratification-dependant diffusivity relies on the parameterization of the vertical diffusion coefficient (K_z) according to the stratification. In the standard version of CLIMBER-2 the vertical diffusion coefficient profile is prescribed. Yet a more physical representation of the diffusion can play a great role for the ocean [*Marzeion et al.*, 2007] and potentially influence the carbon cycle [*Bouttes et al.*, 2009], as the more the ocean is stratified, the more K_z should be reduced. We thus introduce a physical parameterization of the vertical diffusion coefficient K_z depending on the vertical density gradient [*Marzeion et al.*, 2007] in the deep ocean (below 2000 m):

$$K_z = K_0 \left(\frac{N}{N_0}\right)^{-\alpha} \quad (1)$$

where α, K_0 and N_0 are parameters, and $N = \left(-\frac{g}{\rho_0}\frac{\partial\rho}{\partial z}\right)^{\frac{1}{2}}$ is the local buoyancy frequency, with g the gravity acceleration, ρ_0 a reference density, and $\frac{\partial\rho}{\partial z}$ the vertical density gradient. The parameter α controls the sensitivity of the vertical diffusivity to changes in stratification. Its value depends on local conditions and is thus not experimentally constrained on a global scale. In the study we vary α between 0 ($K_z = K_0 = 1. \times 10^{-4}\ m^2/s$) and 1.

[10] The importance of each of the three mechanisms is set by a parameter (*frac*, *iron* and α) between 0 (absence of mechanism) and 1 (maximum mechanism). We realize two ensembles of LGM simulations where the ocean, land and atmosphere carbon and $\delta^{13}C$ reservoirs fully interact

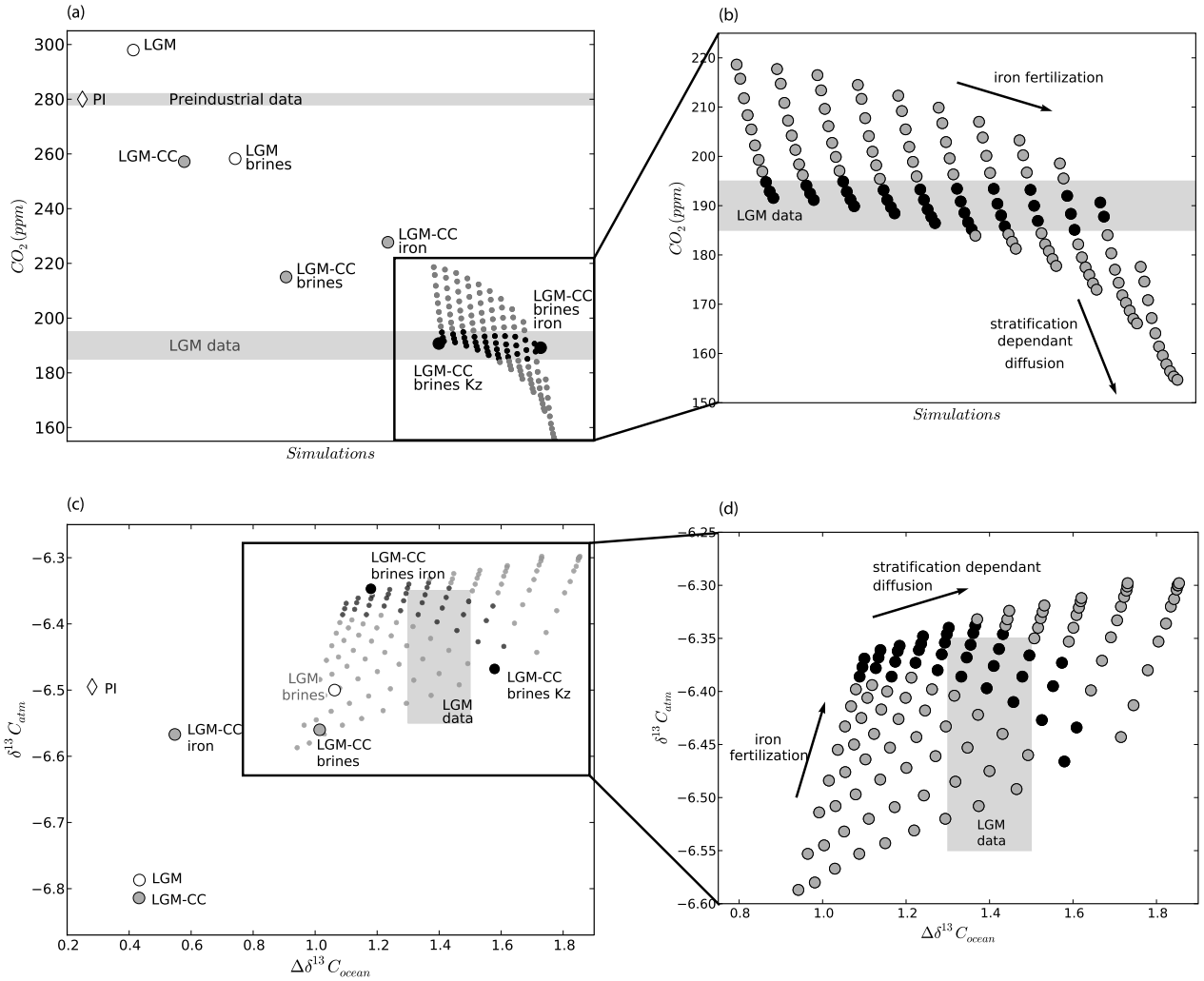

Figure 2. Atmospheric (a and b) CO_2 (ppm) and (c and d) $\delta^{13}C_{atm}$ vs $\Delta\delta^{13}C_{ocean}$ (‰) for LGM simulations with various mechanisms as compared to proxy data. Figures 2a and 2c: *LGM* (standard simulation) and *LGM brines* (with brines: *frac* = 0.6) are without carbonate compensation (CC). All the other simulations take CC into account. *LGM-CC* is the standard simulation with CC, *LGM-CC brines* with brines (*frac* = 0.6) and *LGM-CC iron* with the maximum iron fertilization (*iron* = 1). Two simulations reach the LGM data level: *LGM-CC brines* K_z with brines (*frac* = 0.6) and stratification-dependant diffusion (α = 0.9), and *LGM-CC brines iron* with brines (*frac* = 0.6), and iron fertilization (*iron* = 1). Figures 2b and 2d: zoom for the ensemble of LGM simulations (*frac* = 0.6). The relative importance of iron fertilization (parameter *iron* between 0 and 1) and of the stratification-dependant diffusion (parameter α between 0 and 1) varies in the simulations. Simulations within the range of LGM data are in black. The preindustrial simulation (*PI*) is indicated with a diamond.

to assess the relative importance and role of each of the mechanisms in line with proxy data. In the first one (150 simulations) all parameters vary, which enables us to infer the range of possible values for *frac* (brines) when comparing the results with proxy data. With the second ensemble (120 simulations) the two other parameters only (*iron* and α) vary with better resolution, so that we narrow the range and find nine sets of parameters that match glacial proxy data. We then analyze them to understand the modeled CO_2 drawdown.

3. Results and Discussion

[11] As already studied [*Brovkin et al.*, 2007], the *LGM-CC* simulation gives results that mismatch the data with CO_2 = 257 ppm, $\Delta\delta^{13}C_{ocean}$ = 0.43‰ and $\delta^{13}C_{atm}$ = −6.8‰ compared respectively to 190 ppm, 1.4‰ and −6.45‰ in the data. The addition of the sinking of brines, stratification-dependant diffusion and iron fertilization further decreases CO_2 and increases $\Delta\delta^{13}C_{ocean}$ (Figure 1). The sinking of brines creates a deep isolated oceanic carbon reservoir, mainly because of the stratification induced by the transport of salt as explored by *Bouttes et al.* [2010]. The interactive diffusion amplifies the brine mechanism effects. Because of the enhanced stratification the vertical diffusion coefficient is reduced down to 0.1×10^{-4} m^2/s in the deep (below 3000 m) Atlantic ocean. The vertical mixing is reduced which further isolates the deep water mass. The lower part of the meridional circulation is then less intense.

[12] The first ensemble shows that the *frac* parameter should lie between 0.4 and 1 to match the data. Yet *frac* = 1 is extreme and physically unrealistic as observations indi-

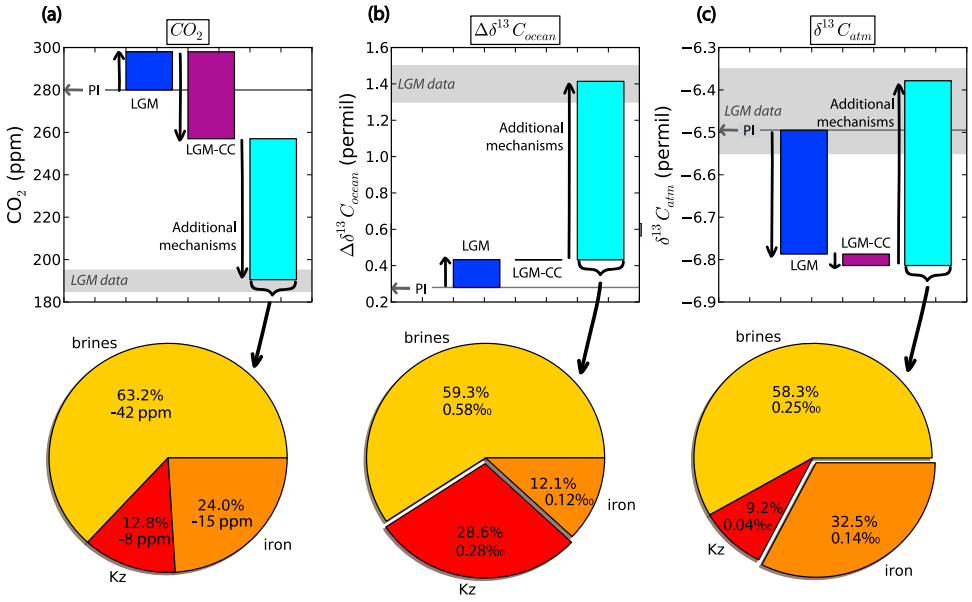

Figure 3. Change of (a) atmospheric CO_2, (b) $\Delta\delta^{13}C_{ocean}$, and (c) $\delta^{13}C_{atm}$ for the control glacial simulation (*LGM*, from the preindustrial simulation *PI*), the glacial simulation with carbonate compensation (*LGM-CC*) and the glacial simulations with all considered mechanisms (mean of the nine simulations that agree best with the data). For the latter, the relative roles of the three additional mechanisms (brine induced stratification (*brines*), stratification-dependant diffusion (K_z) and iron fertilization (*iron*)) are given.

cate that only ~82% of the salt is released into the ocean during sea ice formation [*Haarpaintner et al.*, 2001]. Hence the *frac* range is more probably between 0.4 and 0.8. Such values are supported by modern observations such as measures in the Arctic fjords. Indeed, out of the first rapid salt release of ~82% of the total salt flux, approximately 78% of the brine-enriched shelf water is released out of the fjord in the Norwegian Sea [*Haarpaintner et al.*, 2001], i.e. ~62% of the salt flux rapidly released by sea ice formation.

[13] The second ensemble thus focuses on cases with the median value from the inferred range of *frac* (*frac* = 0.6). We vary the parameters for iron fertilization (*iron*) and the stratification-dependant diffusion (α). In nine of these simulations the model simulates simultaneously the atmospheric CO_2 and $\delta^{13}C$ in agreement with data (Figure 2). To disentangle the effects of these mechanisms we study their impacts when they are alone and in synergy.

[14] The glacial CO_2 level can be reached either with the brine mechanism and stratification-dependant diffusion or with the brine mechanism and iron fertilization. The addition of interactive diffusion to the brine mechanism (*LGM-CC brines* K_z) amplifies its effects. Because of the brine induced stratification, K_z is decreased and the vertical mixing reduced, which further decreases CO_2. Alternatively, iron fertilization associated to the brine mechanism also decreases CO_2 (*LGM-CC brines iron*). Yet the processes involved are different: the stratification-dependant diffusion amplifies the brine effect whereas the iron fertilization effect almost linearly adds to the brine one. However for $\Delta\delta^{13}C_{ocean}$ the two simulations give results that disagree with the data, (respectively ~1.6‰ and ~1.2‰ compared to 1.4‰ in the data). As the data indicate that the "best" simulation should lie between the two considered ones, it clearly appears that both iron fertilization and the stratification-dependant diffusion have a role to play, as it is the case for the nine simulations that match simultaneously the three data values.

[15] For these nine simulations that agree best with the data, we assess the relative role of the three additional mechanisms (brines, stratification-dependant diffusion and iron fertilization) in the CO_2 and $\delta^{13}C$ changes (Figure 3) by successively adding them. The effect of brines alone (*LGM-CC brines*) is a ~42 ppm CO_2 decrease (to 215 ppm). If we add the stratification-dependant diffusion, the additional CO_2 drop is ~8 ppm (between 5 and 12 ppm). With iron fertilization the CO_2 decrease is ~15 ppm (between 10 and 21 ppm). It results that brines play a valuable role both for the CO_2 and $\delta^{13}C$ modifications (around 60%). The other two mechanisms further decrease CO_2, the interactive diffusion appears important mostly for the $\Delta\delta^{13}C_{ocean}$ and iron fertilization for $\delta^{13}C_{atm}$. In addition, our estimated effect for the iron-induced changes in CO_2 (10–20 ppm) lies well within previous estimates based on more complex ocean and biogeochemical models (10–25 ppm) [*Bopp et al.*, 2003; *Tagliabue et al.*, 2009]. The simulated Atlantic $\delta^{13}C$ distribution is in better agreement with data with low values below 3000 m (between 0 and −0.8‰).

4. Conclusion

[16] In conclusion, after accounting for the carbonate compensation, brine mechanism, iron fertilization and stratification-dependant diffusion we can simultaneously reconcile the LGM CO_2 and $\delta^{13}C$. Indeed, not only can we simulate the low glacial CO_2 level of ~190 ppm, but the results are also consistent with the crucial proxy data for the carbon cycle that are $\delta^{13}C$ in the atmosphere and ocean. The brine mechanism plays a major role in this additional change as it accounts for approximately 60% of it. Finally,

the mechanisms involved remain to be tested together in a fully coupled GCM as well as during transitions.

[17] **Acknowledgments.** We thank Alessandro Tagliabue for discussion, Bill Curry and Anna Lourantou for the data, and two anonymous reviewers, the Associate Editor, and Wolfgang Knorr for their comments, which helped improve the manuscript.

References

Archer, D. (1991), Modeling the calcite lysocline, *J. Geophys. Res.*, *96*, 17,037–17,050.

Archer, D., A. Winguth, D. Lea, and N. Mahowald (2000), What caused the glacial/interglacial pCO_2 cycles?, *Rev. Geophys.*, *38*, 159–189.

Berger, A. L. (1978), Long-term variations of daily insolation and Quaternary climatic changes, *J. Atmos. Sci.*, *35*, 2362–2368.

Bird, M. I., J. Lloyd, and G. D. Farquhar (1994), Terrestrial carbon storage at the LGM, *Nature*, *371*, 566.

Bopp, L., K. E. Kohfeld, C. L. Quéré, and O. Aumont (2003), Dust impact on marine biota and atmospheric CO_2 during glacial periods, *Paleoceanography*, *18*(2), 1046, doi:10.1029/2002PA000810.

Bouttes, N., D. M. Roche, and D. Paillard (2009), Impact of strong deep ocean stratification on the carbon cycle, *Paleoceanography*, *24*, PA3203, doi:10.1029/2008PA001707.

Bouttes, N., D. Paillard, and D. M. Roche (2010), Impact of brine-induced stratification on the glacial carbon cycle, *Clim. Past Discuss.*, *6*, 681–710, doi:10.5194/cpd-6-681-2010.

Broecker, W. S., and T.-H. Peng (1987), The role of $CaCO_3$ compensation in the glacial to interglacial atmospheric CO_2 change, *Global Biogeochem. Cycles*, *1*(1), 15–29.

Brovkin, V., A. Ganopolski, D. Archer, and S. Rahmstorf (2007), Lowering of glacial atmospheric CO_2 in response to changes in oceanic circulation and marine biogeochemistry, *Paleoceanography*, *22*, PA4202, doi:10.1029/2006PA001380.

Crowley, T. (1995), Ice age terrestrial carbon changes revisited, *Global Biogeochem. Cycles*, *9*(3), 377–389.

Curry, W. B., and D. W. Oppo (2005), Glacial water mass geometry and the distribution of $\delta^{13}C$ of ΣCO_2 in the western Atlantic Ocean, *Paleoceanography*, *20*, PA1017, doi:10.1029/2004PA001021.

Duplessy, J.-C., N. Shackleton, R. Fairbanks, L. Labeyrie, D. Oppo, and N. Kallel (1988), Deep water source variations during the last climatic cycle and their impact on the global deepwater circulation, *Paleoceanography*, *3*, 343–360.

Fischer, H., et al. (2010), The role of Southern Ocean processes on orbital and millennial CO_2 variations—A synthesis, *Quat. Sci. Rev.*, *29*(1–2), 193–205, doi:10.1016/j.quascirev.2009.06.007.

Haarpaintner, J., J. C. Gascard, and P. M. Haugan (2001), Ice production and brine formation in Storfjorden, Svalbard, *J. Geophys. Res.*, *106*, 14,001–14,013.

Jahn, A., M. Claussen, A. Ganopolski, and V. Brovkin (2005), Quantifying the effect of vegetation dynamics on the climate of the Last Glacial Maximum, *Clim. Past*, *1*, 1–7.

Köhler, P., H. Fischer, G. Munhoven, and R. E. Zeebe (2005), Quantitative interpretation of atmospheric carbon records over the Last Glacial Termination, *Global Biogeochem. Cycles*, *19*, GB4020, doi:10.1029/2004GB002345.

Köhler, P., H. Fischer, and J. Schmitt (2010), Atmospheric $\delta^{13}CO_2$ and its relation to pCO_2 and deep ocean $\delta^{13}C$ during the late Pleistocene, *Paleoceanography*, *25*, PA1213, doi:10.1029/2008PA001703.

Lourantou, A., J. V. Lavric, P. Köhler, J.-M. Barnola, D. Paillard, E. Michel, D. Raynaud, and J. Chappellaz (2010), Constraint of the CO_2 rise by new atmospheric carbon isotopic measurements during the last deglaciation, *Global Biogeochem. Cycles*, *24*, GB2015, doi:10.1029/2009GB003545.

MARGO Project Members (2009), Constraints on the magnitude and patterns of ocean cooling at the Last Glacial Maximum, *Nat. Geosci.*, *2*, 127–132, doi:10.1038/ngeo411.

Martin, J. H. (1990), Glacial-interglacial CO_2 change: The iron hypothesis, *Paleoceanography*, *5*, 1–13.

Marzeion, B., A. Levermann, and J. Mignot (2007), The role of stratification-dependent mixing for the stability of the Atlantic overturning in a global climate model, *J. Phys. Oceanogr.*, *37*, 2672–2681, doi:10.1175/2007JPO3641.1.

Monnin, E., A. Indermühle, A. Daellenbach, J. Flueckiger, B. Stauffer, T. F. Stocker, D. Raynaud, and J.-M. Barnola (2001), Atmospheric CO_2 concentrations over the Last Glacial Termination, *Science*, *291*, 112–114.

Paillard, D., and F. Parrenin (2004), The Antarctic ice sheet and the triggering of deglaciations, *Earth Planet. Sci. Lett.*, *227*, 263–271.

Peltier, W. R. (2004), Global glacial isostasy and the surface of the ice-age Earth: The ICE-5G (VM2) model and GRACE, *Annu. Rev. Earth Planet. Sci.*, *32*, 111–49, doi:10.1146/annurev.earth.32.082503.144359.

Petoukhov, V., A. Ganopolski, A. Eliseev, C. Kubatzki, and S. Rahmstorf (2000), CLIMBER-2: A climate system model of intermediate complexity, part I: Model description and performance for present climate, *Clim. Dyn.*, *16*, 1–17.

Sigman, D. M., and E. A. Boyle (2000), Glacial/interglacial variations in atmospheric carbon dioxide, *Nature*, *407*, 859–869, doi:10.1038/35038000.

Sigman, D. M., M. P. Hain, and G. H. Haug (2010), The polar ocean and glacial cycles in atmospheric CO_2 concentration, *Nature*, *466*, 47–55, doi:10.1038/nature09149.

Tagliabue, A., L. Bopp, D. M. Roche, N. Bouttes, J.-C. Dutay, R. Alkama, M. Kageyama, E. Michel, and D. Paillard (2009), Quantifying the roles of ocean circulation and biogeochemistry in governing ocean carbon-13 and atmospheric carbon dioxide at the Last Glacial Maximum, *Clim. Past*, *5*, 695–706.

Toggweiler, J. R. (1999), Variation of atmospheric CO_2 by ventilation of the ocean's deepest water, *Paleoceanography*, *14*, 571–588.

L. Bopp, N. Bouttes, and D. Paillard, Laboratoire des Sciences du Climat et de l'Environnement, IPSL/CEA-CNRS-UVSQ, Orme des Merisiers, Gif-sur-Yvette, F-91191, France. (nathaelle.bouttes@lsce.ipsl.fr)

V. Brovkin, The Land in the Earth System, Max-Planck-Institute for Meteorology, Bundesstr. 55, Hamburg, D-20146, Germany.

D. M. Roche, Section Climate Change and Landscape Dynamics, Faculty of Earth and Life Sciences, Vrije Universiteit Amsterdam, De Boelelaan 1085, NL-1081 Amsterdam, Netherlands.